PROCEEDINGS, 41st Workshop on Geothermal Reservoir Engineering
Stanford University, Stanford, California, February 22-24, 2016
SGP-TR-209

Gigawatt-Scale Power Potential of a Magma-Supported Geothermal System in the Fold and Thrust Belt of Southeast Idaho

John A. Welhan

Idaho Geological Survey, Dept. of Geosciences, Idaho State University, Pocatello, Idaho 83209-8072

welhjohn@isu.edu

Keywords: high-temperature, sedimentary, geothermal resource potential

ABSTRACT

Allis and coworkers (Allis et al., 2012; 2013; 2015) have made a strong case that hot stratigraphic geothermal reservoirs could host considerable thermal energy within an economic temperature-depth window of 150 to 200 ^{o}C at 2 to 4 km. One such area has been identified in Idaho's fold and thrust belt (Welhan et al., 2014) and was evaluated to provide a first-order appraisal of its stored thermal energy and electric power-generating potential. Elevated heat flows, determined from data in more than 30 deep oil and gas exploration wells that have been drilled in Idaho's thrust belt (Welhan and Gwynn, 2014), range from 90 to >120 mW/m^2, with depths of 2.5 to 3.3 km to the 150 ^{o}C isotherm and corrected bottom-hole temperatures in excess of 220 ^{o}C in the most favorable area. Potential reservoir rocks known to be oil and gas producers in northern Utah, which also host productive aquifers in the study area, were encountered in all deep wells drilled in the high-heat flow areas. The aggregate thickness of potential reservoir rocks is estimated at 100 to 700 meters within the 250 to 500 km^2 area of highest heat flow, where four boreholes have temperatures of 185 to 240 ^{o}C at 4 km depth.

Using the stored-heat method and a range of thermal recovery and energy conversion factors representative of geothermal power plants worldwide, the median electric power-generating potential of the area of highest-heat flow is estimated at 1 to 1.3 GW$_e$. An area of moderately elevated heat flow and lower reservoir temperatures, with depths of 4 to 4.2 km to the 150 ^{o}C isotherm, has 75 to 90 MW$_e$ of power-generation potential, but the greater depths and high fluid salinities suggest that development potential in this area is marginal. A third area, defined by a single high heat-flow well with reservoir temperatures of 150-195 ^{o}C at depths between 3.1 and 4 km, appears to be the best prospect for near-term development. It is located within 25 km of the phosphate mining and processing center of Soda Springs and less than 10 km from a regional high-voltage transmission corridor. The power-generating potential in the vicinity of this well is conservatively estimated at a minimum of 160 to 200 MW$_e$ or higher, depending on how large a reservoir area is eventually delineated.

1. INTRODUCTION

A previously unrecognized high-temperature geothermal resource in Idaho's fold and thrust belt has been identified on the basis of deep oil and gas exploration well data (Welhan and Gwynn, 2014) and its structural relationship to a nearby late-Quaternary rhyolite magma (McCurry and Welhan, 2012; McCurry et al., 2015). Geologic conceptual models of the resource indicate that the most likely heat transport mechanism is advective transfer from the magmatic heat source at ca. 12-14 km depth into sedimentary reservoir rocks at 3-5 km depth (Welhan et al., 2014; Welhan, in review).

Despite considerable early interest in this area's geothermal potential (Mitchell et al., 1980; IDWR, 1980) and initial estimates of residual thermal energy associated with its youthful magma chamber (Smith et al., 1978; Smith and Shaw, 1979), exploration interest all but disappeared for lack of any evidence of a high-temperature resource, including a 2.4 km exploration hole drilled in the Basin and Range graben adjacent to 57 ka rhyolite domes of the Blackfoot volcanic field. Renewed interest emerged recently with the synthesis of deep-well data compiled for the National Geothermal Data System (Welhan et al., 2013a, 2013b, 2014). This work culminated in the development of conceptual models of a hot sedimentary geothermal system (Welhan, in review), which hosts a thermal resource at economically drillable depths, of the type that Allis et al. (2013, 2014) and others have championed.

This communication summarizes relevant data on heat flow, temperatures, and potential reservoir rocks in this area of the Idaho thrust belt and utilizes those data to estimate the stored thermal energy and electric power-generating potential of the best-characterized part of this system. Care has been taken to be as conservative as possible in estimating reservoir volumes and temperatures and to use thermal recovery and energy conversion factors that reflect actual values characteristic of operating geothermal power production facilities.

2. GEOLOGIC CONTEXT

The location of the geothermal resource and its relationship to the Blackfoot volcanic field (BVF) are shown in **Figure 1**. The BVF is a complex of Quaternary-age basalt and rhyolite volcanic rocks located in the northeastern-most part of the Basin and Range (B&R) province where it transitions into the Idaho thrust belt (ITB). Three major B&R grabens were filled with tholeiitic basalt of a composition similar to that of the eastern Snake River Plain (ESRP), creating a volcanic field that extends from about 20 to 90 km south of the ESRP's southern margin. China Hat, the largest rhyolite dome of two major dome fields, with a surface volume of ca. 0.7 km^3 (Ford, 2005), is located in the central graben (**Figure 1**). It erupted at 57 ka from a parent magma ca. 12-14 km deep (as constrained by hornblende thermobarometry; Ford, 2005). An earlier dome field 25 km NNE of China Hat (Figure 1) erupted at 1.5 Ma (McCurry and Welhan, 2012).

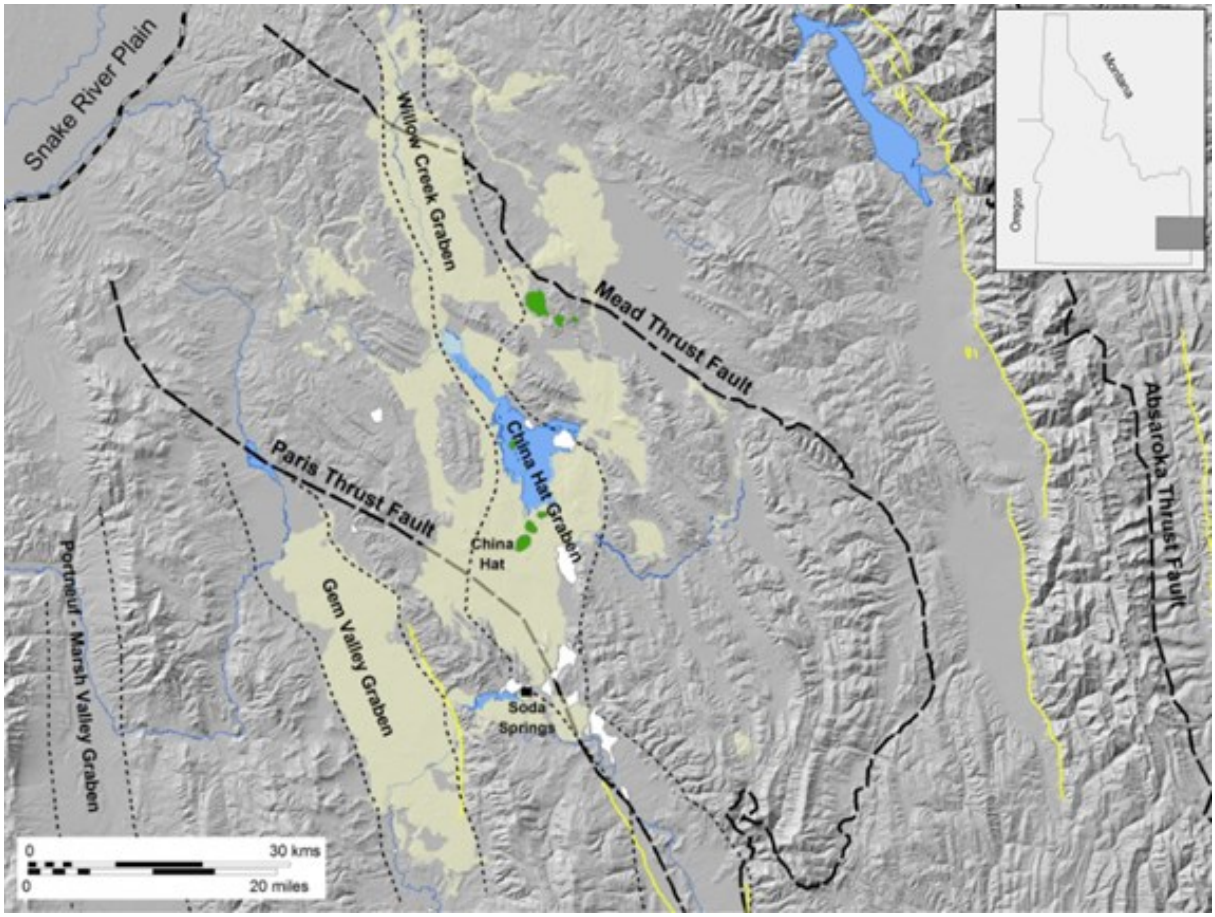

Figure 1: Location of study area in the Idaho thrust belt, showing major thrust faults, Basin and Range grabens (lightly dashed lines) and the areal extent of the Blackfoot volcanic field (lightly shaded). Green polygons indicate northern (1.5 Ma) and southern (57 ka) rhyolite dome fields and the location of the China Hat dome. White polygons represent mapped travertine terraces in the area, and faults with Quaternary activity are shown in yellow.

Figure 2 summarizes cross sections of the Idaho thrust belt (ITB) in the vicinity of the geothermal resource, based on balanced sections constructed by Dixon (1982) and constrained by well control and hundreds of miles of seismic line data. **Figure 3** summarizes the crustal framework and known reservoir rocks of the thrust belt, including the ITB. Some 40 km of Archean to early Proterozoic crust is overlain by 6-10 km of late Proterozoic to Mesozoic carbonates, clastics and evaporites that were stacked eastward in extensive thrust sheets during Laramide, Sevier and older orogenies. Rocks of the Absaroka thrust plate, in which the geothermal reservoirs occur, are of Mississippian to Cretaceous age, with pre-Cretaceous rocks having a total conformable thickness of approximately 7300 m. This interval is also where most of the productive oil and gas reservoirs of the Utah-Wyoming thrust belt occur (Figure 3). Lithologies of pre-Cretaceous rocks are predominantly limestone, shale and siltstone/sandstone, approximately in that order of relative abundance. Basin and Range normal faulting began in the mid-Miocene in response to east-west extension and interaction with the Yellowstone-ESRP hot spot track, and the resulting magmatic phase extended from the late Pliocene to the present (Ford, 2005; McCurry and Welhan, 2012).

3. THERMAL CONTEXT

Welhan and Gwynn (2014) synthesized bottom-hole temperature (BHT) and drill stem test (DST) data compiled for the National Geothermal Data System (NGDS) in order to calculate heat flow for 31 oil and gas exploration wells drilled in the Idaho thrust belt (ITB) in the vicinity of the BVF. Several BHT correction methods were compared against DST data and an aggregate average of the best methods was applied. Formation-specific thermal conductivity estimates were also compiled and evaluated in order to improve the accuracy of the heat flow estimates.

Tables 1 and **2** summarize the boreholes and results from Welhan and Gwynn (2014). Their heat flow estimates were calculated in two ways: (i) as the product of the average borehole gradient and formation thermal conductivity averaged over the length of the borehole, and (ii) a fitted conductive geotherm model, based on estimated formation-specific thermal conductivities and thicknesses.

4. METHODOLOGY

4.1 Estimation Procedure

The challenge in geothermal resource assessment at this stage is to estimate the volumetric size of the resource and its stored thermal energy content, identify practical constraints on extracting and converting that energy to electric power, and estimate the uncertainties in the derived estimates of electric power capacity. The amount of electric energy recoverable from a geothermal reservoir depends on theamount of thermal energy in the reservoir, the fraction which is extractable at the wellhead, and the efficiency of converting thermal energy to electric energy for the fluid temperatures and energy-conversion process that is utilized.

Two different approaches have been used to estimate power production potential from a geothermal reservoir: the production simulation method, whereby the recovery rate of fluid from production wells is modeled to predict the rate at which thermal energy can be produced from the reservoir; and the stored heat or volumetric method, which estimates the thermal energy content of the reservoir and reduces that by the fraction that is practically recoverable and by the thermodynamic efficiency of converting thermal to electric energy (Nathenson, 1975; Muffler, 1979; Williams et al., 2008).

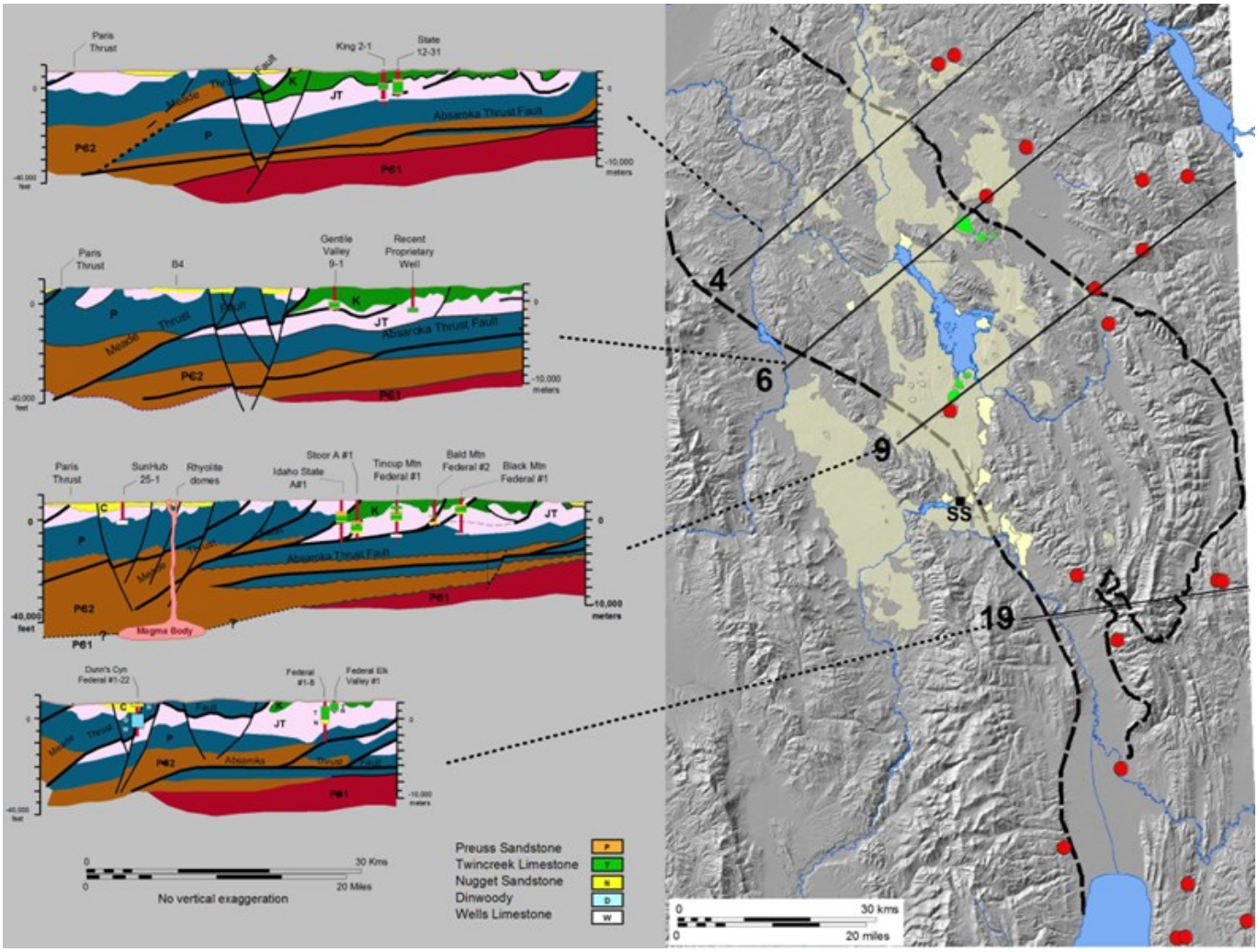

Figure 2: Locations of selected cross sections constructed from seismic and well data in the Idaho thrust belt, after Dixon (1982). Red dots represent locations of deep oil and gas exploration well control data; light green polygons indicate northern and southern rhyolite dome fields; white polygons represent mapped travertine terraces in the area; "SS" = town of Soda Springs.

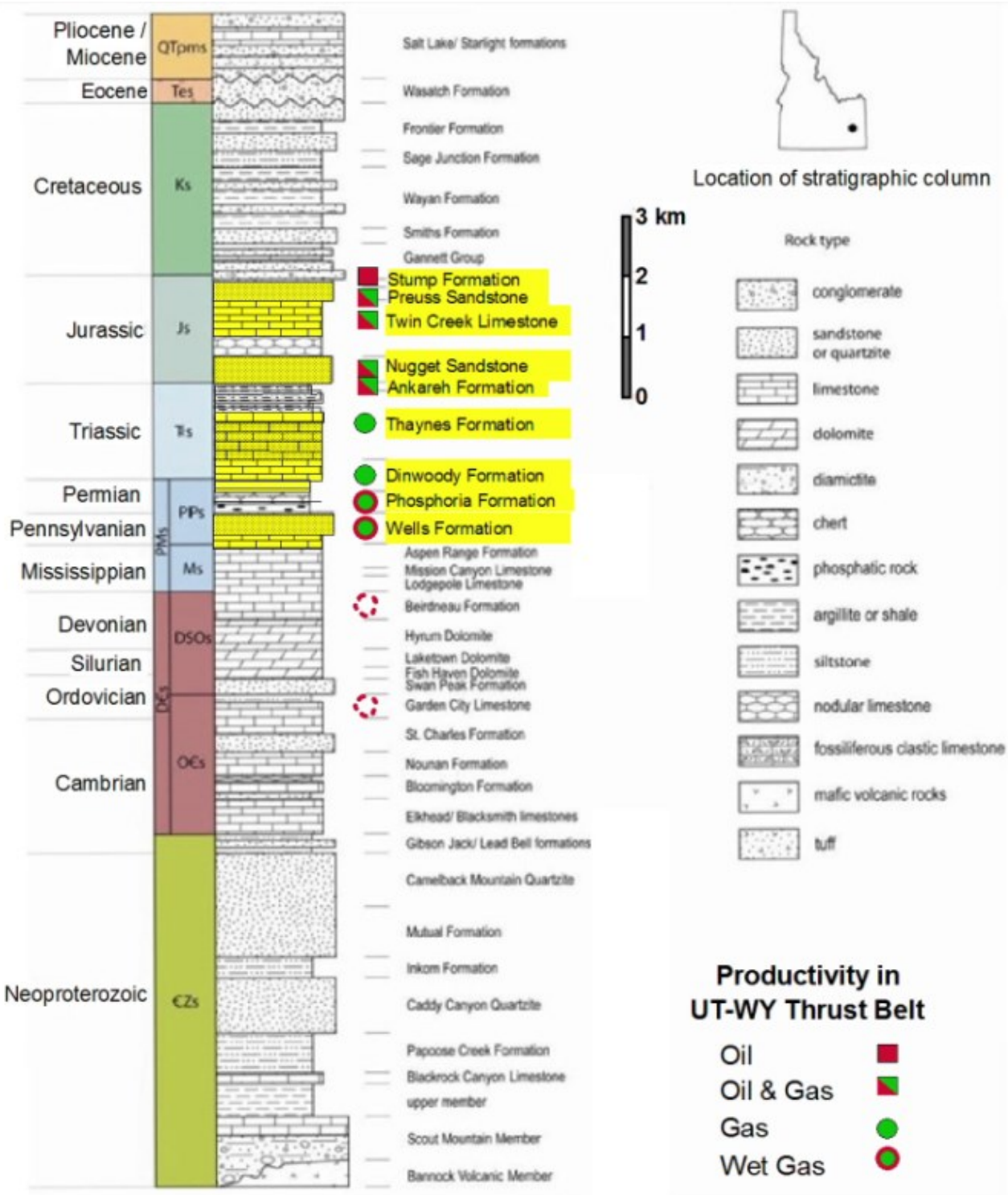

Figure 3: Generalized stratigraphy of the Idaho thrust belt, showing productive reservoir rocks in the Utah-Wyoming thrust belt (Powers, 1983; dashed red circles indicate formations outside of Idaho). Productive oil and gas reservoirs are generally restricted to Jurassic to Pennsylvanian formations. Modified from Lewis et al. (2012).

API	Well Name	Operator	Latitude[2]	Longitude[2]	Surface Elevation, m	Total Depth, m	Spud Date	End Date
11-07-20019	Archie Parker No. 1	Texaco	42.30514	-111.45305	1882	3051	3-Jan-1988	19-Mar-1988
11-19-20003	Bald Mountain No. 1	Amoco Production Co.	43.10484	-111.20103	2495	2768	1-Aug-1983	5-Nov-1983
11-19-20004	Bald Mountain No. 2	Amoco Production Co.	43.10512	-111.22446	2370	4314	6-Jul-1981	18-Apr-1982
11-07-20008	Bennington No. 3-24	Ladd Petroleum	42.40377	-111.42060	2001	4124	5-Oct-1979	1-Mar-1980
11-07-20007	Big Canyon Federal No. 1-13	Union Texas Petroleum	42.54825	-111.37449	2070	3570	12-Sep-1978	15-Mar-1979
11-19-20001	Black Mountain Federal No.1	American Quasar Petroleum Co.	43.10924	-111.13688	2495	4368	17-Aug-1976	27-Mar-1977
11-29-00000[1]	Dry Valley No. 1	Standard Oil of Calif.	42.77624	-111.33418	2060	2398	8-Jul-1952	5-Dec-1952
11-07-20013	Dunn's Canyon Federal No. 1-22	Chevron USA Inc.	42.45284	-111.30293	2134	4129	1-Dec-1980	17-Sep-1981
11-07-20012	Federal DI No. 1	Cities Service Co.	42.10327	-111.18099	1940	3128	10-Feb-1981	21-Jun-1981
11-29-20001	Federal Elk Valey No. 1	May Petroleum Inc.	42.53241	-111.09520	2284	1195	14-Jul-1976	19-Aug-1976
11-29-20004	Federal No. 1-8	May Petroleum Inc.	42.57053	-111.10517	2343	5105	15-Jul-1977	27-Sep-1978
11-19-20002	Gentile Valley No. 1-9	Continental Oil Co.	43.08935	-111.53288	2080	3021	20-Sep-1978	16-Aug-1979
11-19-00000[1]	Government No. 1	Edwin Allday	43.39756	-111.21326	1699	1756	3-Sep-1965	1-Mar-1966
11-07-20006	Grace Federal No. 10-1	American Quasar of New Mexico	42.04858	-111.07010	2325	3615	21-Feb-1978	20-Aug-1978
11-11-20002	Hoff No. 1-8M	Union Oil Co. of Calif.	43.34336	-111.91790	1753	2726	22-May-1979	30-Oct-1979
11-29-20006	Idaho State "A" No. 1	Phillips Petroleum Co.	42.90278	-111.29906	2038	4963	12-Feb-1981	30-Sep-1982
11-07-20005	Jensen No. 22-1	American Quasar of New Mexico	42.27151	-111.30341	1812	3591	1-Sep-1977	27-Jan-1978
11-11-20001	King No. 2-1	American Quasar of New Mexico	43.27615	-111.61489	2012	4132	3-Feb-1978	22-Aug-1978
11-07-20010	N. Eden Federal No. 21-11	American Quasar	42.02776	-111.20460	2114	2862	24-Dec-1979	31-May-1980
11-07-20011	N. Rabbit Creek Federal No. 6-21	American Quasar	42.06598	-111.12355	2055	3537	19-Jan-1980	24-Jul-1980
11-07-20009	Rigby "A" Williams No. 1	Cities Service	42.25843	-111.09936	1899	3360	25-Oct-1979	5-Mar-1980
11-07-00000[1]	Sheep Creek No. 1	Standard of Calif.	42.07952	-111.18723	1986	2063	24-May-1952	18-Dec-1952
11-19-20005	State No. 12-31	Juniper Petroleum Co.	43.29111	-111.58472	2057	2981	18-Jul-1981	16-Oct-1981
11-29-20005	Stoor "A" No. 1	Phillips Petroleum Co.	42.95347	-111.32313	2059	4605	23-Dec-1979	15-Jan-1980
11-07-20015	Sweetwater No. 5-13	Sohio Petroleum Co.	42.05552	-111.10904	2041	3541	2-Sep-1983	20-Jan-1984
11-19-20007	Tincup Mountain Federal No. 1	Sun Exploration and Production Co.	43.01061	-111.22467	2456	5060	19-Sep-1984	14-Jun-1985
11-19-00000[1]	USA-TJ Weber No. 1-A	Pan American Petroleum	43.22928	-111.26237	2428	2962	29-Sep-1963	29-Oct-1964
11-29-00000[1]	USA-Wild No. 1	Amerada Petroleum	42.52566	-111.08490	2285	1254	25-Aug-1963	13-Oct-1963
11-07-20016	Worm Creek No. 1	Murphy Oil	42.16149	-111.41771	1846	2284	17-May-1984	23-Jul-1984
11-19-20011	CPC 17-1	CPC Minerals, LLC	43.15767	-111.44868	1954	2885	1-Sep-2007	6-Dec-2001
11-29-30001	SunHub 25-1	Hunt Oil Co.	42.78670	-111.61170	1890	2373	5-Oct-1979	1-Mar-1980

[1] Well identifier not assigned

[2] WGS 1984

Table 1: Summary of deep oil and gas exploration wells having thermal data that was used to calculate corrected BHTs and best available heat flow estimates. After Welhan and Gwynn (2014).

Following standard practice (e.g., Mendrinos et al., 2008; Franz et al., 2015), the stored thermal energy, E_R, of a reservoir can be estimated as

$$E_R = C_R V_R (T_R - T_o), \quad (1)$$

where C_R is the volumetric specific heat of reservoir rock plus water (ca. 2450 kJ/m^3, for 10% porosity), V_R is the volume of the reservoir, T_R is reservoir temperature, and T_o is the rejection or base temperature, typically that of ambient air or the condenser temperature (Brook et al., 1979). The value of T_o is important in determining the amount of useful work that can be extracted and the thermodynamic efficiency of energy conversion (Franz at al., 2015). In this evaluation, three T_o scenarios were considered: T_o =15 ^{o}C; T_o =40 ^{o}C (Garg and Combs, 2011); and T_o variable between 15 and 40 ^{o}C.

The extractable amount of thermal energy, E_X, depends on the thermal recovery factor, R, defined as

$$R = E_x / E_R. \quad (2)$$

Data from producing hydrothermal reservoirs indicates that R is effectively in the range of ca. 0.02 to 0.1 (Sanyal et al., 2002; Sanyal and Sarmiento, 2005), depending on the thermal influences of heterogeneities and reservoir flow characteristics that dictate efficiency of fluid extraction from the reservoir. This range is more conservative than that assumed by Williams et al. (2008) and the approach utilized in the GeoFRAT tool (EGI, 2014).

The available electrical energy (E_e) that can be derived from the extractable thermal energy depends on power plant design (thermodynamic and operating characteristics) and environmental factors such as the rejection temperature (T_o) and its seasonal variability. The energy conversion efficiency (n) is defined as the ratio of electric energy produced by a power plant to the thermal energy delivered to it:

$$n = E_e / E_x \quad (3)$$

and the installed power-generating capacity of the plant, P_e, is

$$P_e = E_e / (F \cdot t), \quad (4)$$

where F is a capacity factor (fraction of time that a plant produces power, typically 0.9 for a base load power plant), and t is the plant's operating life, assumed to be 30 years. Based on an analysis of 94 steam-powered (dry and flashed-steam) power plants worldwide, Moon and Zarrouk (2012) determined the average energy conversion efficiency (n) to be 0.12, including parasitic energy losses. In

comparison, the average conversion efficiency based on data from 31 operating binary plants worldwide ranged from 0.05 to 0.08 at reservoir temperatures of 150 to 220 °C, respectively.

Well Name	Data Type	Corrected Temperature Depth, m[1]	Temperature, °C Corrected[2]	Temperature, °C Surface[3]	Overall Corrected Gradient, °C/km[4]	Average Thermal Conductivity, W/m·°K[5]	Heat Flow (mW/m²)[6]	Modeled Heat Flow (mW/m²)[7]
Archie Parker No. 1	BHT	3041	87.0	7.6	26.1	3.1	81	75
Bald Mountain No. 1	BHT	2749	94.4	4.5	32.7	3.2	104	100
Bald Mountain No. 2	BHT	3832	140.0	4.5	35.4	2.6	91	85
Bennington No. 3-24	BHT	4127	97.3	6.9	21.9	2.8	62	50
Big Canyon Federal No. 1-13	BHT	3577	172.4	6.4	46.4	2.5	117	116
Black Mountain Federal No.1	BHT	4159	120.3	3.7	28.0	2.5	70	70
Dry Valley No. 1	BHT	1903	51.4	6.5	23.6	2.7	64	65
Dunn's Canyon Federal No. 1-22	BHT	4079	147.3	6.0	34.6	2.8	97	93
Federal DI No. 1	BHT	3056	80.6	7.2	24.0	2.6	62	60
Federal Elk Valley No. 1	BHT	967	36.8	5.0	32.9	2.8	93	93
Federal No. 1-8	BHT	5104	167.1	4.6	31.8	2.6	84	80
Gentile Valley No. 1-9	BHT	3008	161.8	6.3	51.7	2.6	136	129
Government No. 1	DST	405	21.1	8.8	30.4	2.7	82	67
Grace Federal No. 10-1	BHT	3616	85.2	4.8	22.2	2.7	61	58
Hoff No. 1-8M	BHT	2721	102.5	8.4	34.6	2.5	86	85
Idaho State "A" No. 1	BHT	4979	183.4	6.6	35.5	2.9	102	98
Jensen No. 22-1	BHT	3499	96.6	8.1	25.3	2.7	67	57
King No. 2-1	BHT	4069	202.2	6.8	46.9	2.4	114	107
N. Eden Federal No. 21-11	DST	3190	84.4	6.1	24.6	2.6	63	64
N. Rabbit Creek Federal No. 6-21	BHT	3538	87.5	6.5	22.9	2.7	63	59
Rigby "A" Williams No. 1	DST	3347	75.0	7.5	20.2	2.5	50	50
Sheep Creek No. 1	BHT	2053	56.2	6.9	24.0	2.6	62	57
State No. 12-31	BHT	2965	116.9	6.5	37.2	2.6	99	92
Stoor "A" No. 1	BHT	4510	192.4	6.5	41.2	2.3	95	91
Sweetwater No. 5-13	BHT	3538	88.3	6.6	23.1	2.9	68	64
Tincup Mountain Federal No. 1	BHT	5056	179.5	3.9	34.7	2.9	101	93
USA-TJ Weber No. 1A	BHT	2964	155.3	4.1	51.0	2.7	138	132
USA-Wild No. 1	DST	1229	50.6	5.0	37.1	2.6	98	91
Worm Creek No. 1	BHT	2284	58.5	7.8	22.2	2.4	53	50
CPC 17-1	BHT	2865	160.3	7.1	79.7	2.7	165	160
SunHub 25-1	BHT	2373	80.1	7.6	30.5	2.7	82	79

[1] Based on deepest corrected BHT or reliable DST.
[2] Reliable corrected BHT or DST (see text).
[3] Mean annual surface temperature + 3°C (see text).
[4] Gradient based on deepest reliable corrected BHT or DST and calculated surface temperature.
[5] Average of thermal conducivity values used in geotherm models.
[6] Heat flow calculated by multiplying the average thermal conductivity and the overall geothermal gradient.
[7] Heat flow calculated using geotherm models.

Table 2: Summary of heat flows calculated from deep oil and gas well data, after Welhan and Gwynn (2014).

The choice of an appropriate energy-conversion method (single- or double-flash steam vs. binary-cycle process) depends on reservoir temperature and the chemical nature of its fluids, including scaling, corrosion, and environmental considerations, among other things. Single-flash steam power plants operate over the widest range of reservoir enthalpies, from ca. 800 to 2800 kJ/kg (> 190 °C for pure water), but steam production from high-salinity fluids can be problematic from engineering and environmental perspectives. Double-flash steam plants are more efficient up to fluid enthalpies of ca. 1900 kJ/kg (Moon and Zarrouk, 2012), and the binary plants evaluated by those authors operated economically from ca. 300 to 1000 kJ/kg (equivalent to temperatures of 75 to 230 °C for pure water). Considering the temperature range of ITB fluids, a binary-cycle process would be the logical choice where elevated salinities exist, whereas a flashed-steam process would be more efficient for developing low- to moderate-salinity fluids.

Combining equations (1) through (4) yields an expression for the power plant's electric-generation capacity in terms of the thermal reservoir's volume and temperature (Mendrinos et al., 2008):

$$Pe = n \cdot R \cdot C_R \cdot V_R \cdot (T_R - T_o) / (0.2778 \cdot F \cdot t), \quad (5)$$

where 0.2778 is a conversion factor for kiloJoules to Watt-hours.

In contrast to the thermal recovery and energy conversion factors utilized in GeoFRAT (EGI, 2014; Williams et al., 2008), the ranges of both variables in the present analysis are set significantly lower, based on values documented in operating geothermal fields: based on 52 flashed-steam and 31 binary power plants worldwide (Moon and Zarouk, 2012), values of n between 0.05 and 0.12 were assumed for a flashed-steam process and between 0.05 and 0.08 for a binary-cycle process, and R was conservatively set at 0.02 to 0.1 (Sanyal et al., 2002; Sanyal and Sarmiento, 2005). The volumetric heat capacity (C_R = 2450 kJ/m^3) represents an assumed porosity of 10% in a limestone or sandstone reservoir. Rejection temperatures (T_o) of up to 40 °C were considered in this analysis (Brook et al. 1979). Higher rejection temperatures may be necessary to avoid scaling issues, particularly if the ITB's deep brines are developed (e.g., Kalinci et al., 2014).

4.2 Reservoir Temperature and Volume

The areal extent of the ITB's thermal anomaly was estimated by indicator kriging of the deep-well heat-flow measurements and using the probability of exceeding a heat-flow threshold of 110 mW/m^2 (Welhan and Gwynn, 2014; Welhan, in review) as the criterion for estimating the area of the resource (**Figure 4**). Given the geologic complexity of thrust belt rocks which host this thermal resource and the relative paucity of deep-well data, this estimate is necessarily approximate, at 500 km^2. Similarly, the thickness and spatial extents of its thermal reservoirs can only be crudely estimated. At this stage in the resource evaluation process, therefore, it is possible only to place approximate bounds on the volume and average temperature. Available borehole data indicates the maximum temperature in the

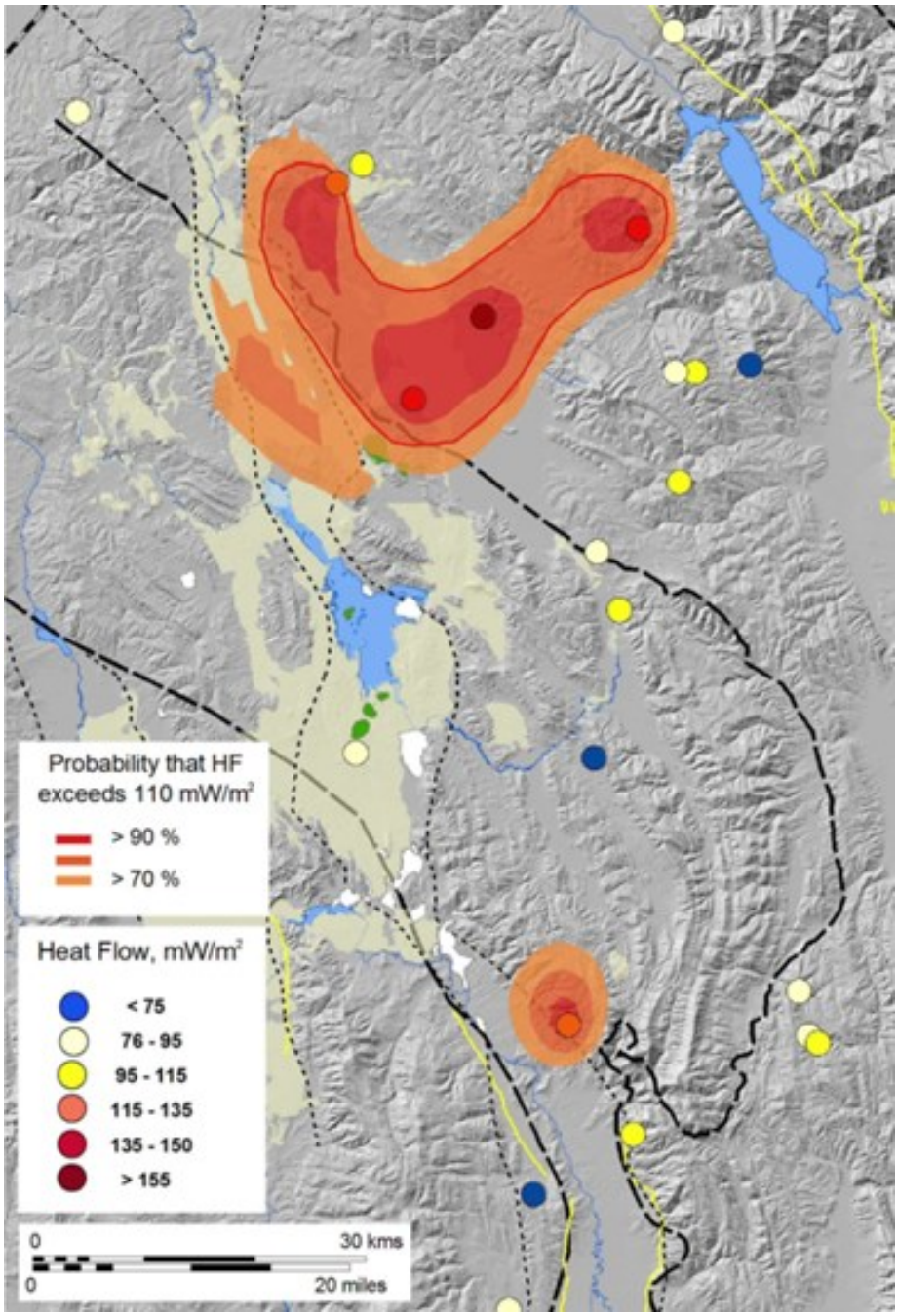

Figure 4: The spatial distribution of elevated heat flow as determined from deep well thermal data, after Welhan and Gwynn (2014) and interpolated with indicator kriging to show the probability that heat flow exceeds 110 mW/m^2. The probability color scale is restricted to probabilities >70% so as to highlight the highest heat flow areas. For reference, the primary heat flow anomaly having ≥ 80% likelihood of exceeding 110 mW/m^2 has an area of 500 km^2 (red polygon). After Welhan (in review).

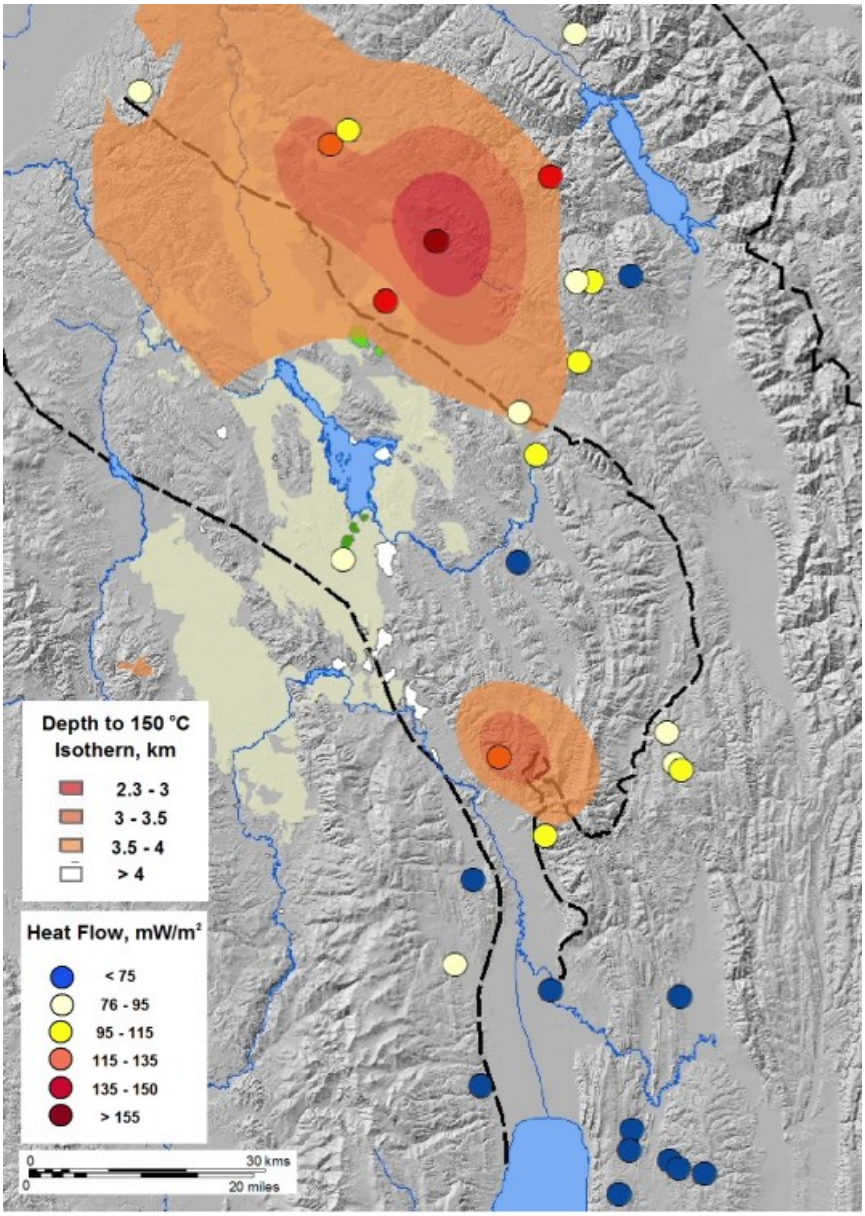

Figure 5: Kriging-interpolated depths to the 150 °C isotherm, as determined from deep-well data of Welhan and Gwynn (2014) and their modeled thermal gradients. After Welhan (in review).

ITB is greater than 220 °C. Based on interpolated isotherm depths (**Figure 5**), T_R is estimated to range from a minimum of 150 °C at 5 km depth in Area C to as much as 240 °C at 4 km depth within Areas A and B (Welhan, in review).

Figure 6 shows the three areas for which power generation estimates were calculated. The maximum extent of Area A is assumed to correspond to the 80% probability contour of exceeding 110 mW/m^2, as indicated by the red polygon in Figure 4 (500 km^2). In order to be as conservative as possible, its minimum area was arbitrarily set at half this value (250 km^2). The extent of Area B is defined by the 80% probability contour of exceeding 110 mW/m^2 and Area C's extent is arbitrarily defined by a rectangle drawn around five wells southeast of Area A that intercept the 150 °C isotherm at depths of 4-4.2 km. The volume and average temperature of reservoir rock within each area is estimated from the cumulative thickness of known reservoir-quality formations between the 150 °C isotherm and an assumed maximum drillable depth of 4 km in Areas A and B (Allis et al., 2012; 2014) and a depth of 5 km in Area C. The depth to the 150 °C isotherm in Areas A and B is of the order of 2.4 to 3.3 km, compared with 4 to 4.2 km in Area C. Temperatures, depths and reservoir thickness estimates for Areas A and B are quite similar, suggesting that the power-generation potential of Area B may be substantially larger than that based on the area shown in Figure 6, which is defined by a single well.

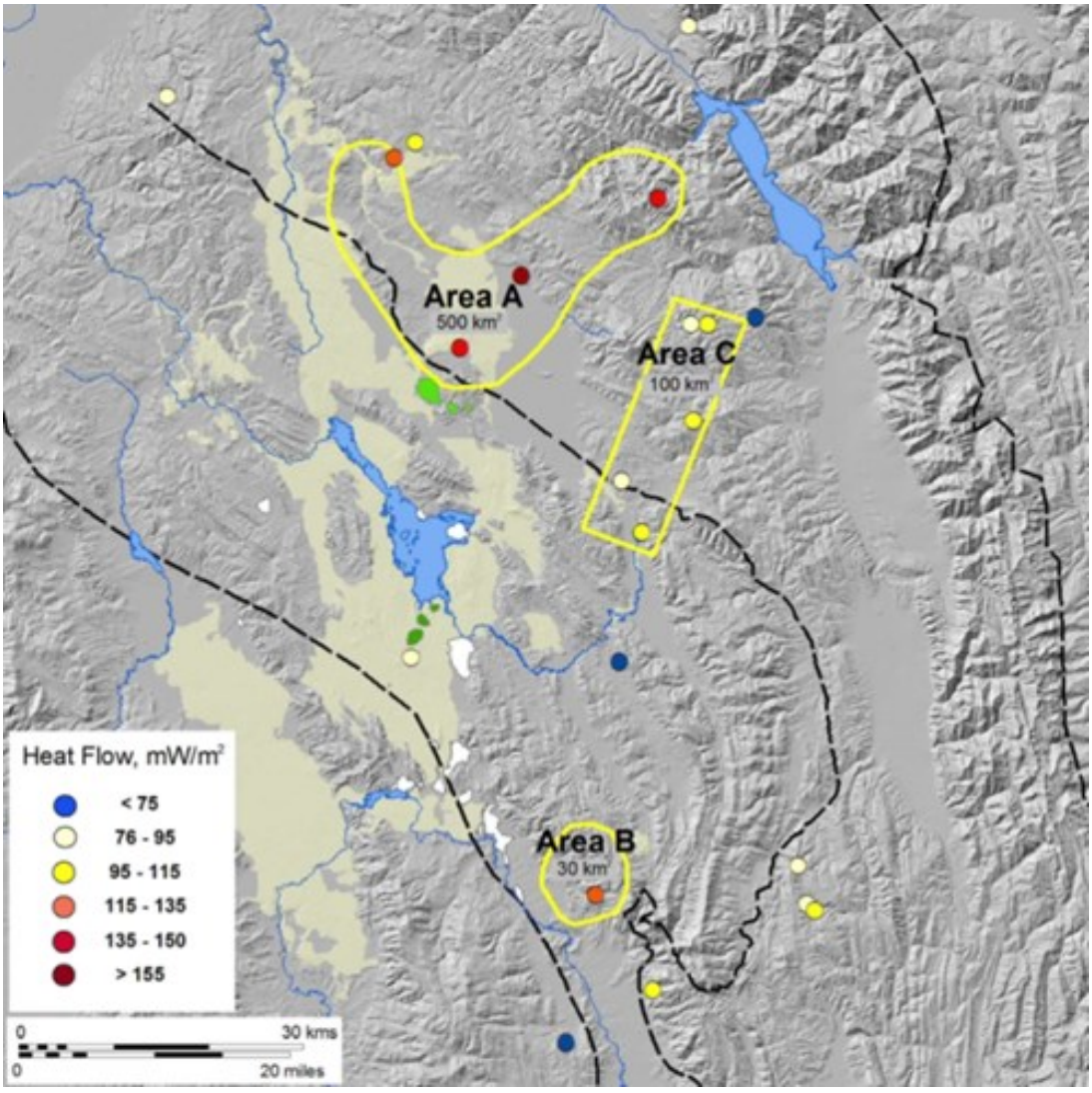

Figure 6: Areas that have higher than background heat flow in the Idaho thrust belt for which power generation potential was estimated in this paper. Area A and Area B are defined on the basis of an 80% probability of exceeding 110 mW/m^2 heat flow, whereas Area C is arbitrarily defined by a bounding rectangle around wells having moderately elevated heat flow. Corresponding areas of each polygon are shown. Heat flow data are from Welhan and Gwynn (2014). Other symbology as in Figure 1.

Relevant formation tops data on all wells in the three areas are plotted in **Figure 7**, showing potential reservoir rocks that were encountered in each well, together with the fitted thermal profiles of Welhan and Gwynn (2014). **Table 3** summarizes relevant isotherm depths, reservoir thicknesses and temperatures for the three areas. Figure 7 depicts principal reservoir-quality formations known to be productive oil and gas producers in the Utah-Wyoming thrust belt (Figure 3), as well as formations and lithologies known to host prolific shallow aquifers in the study area (Welhan, in review). The effective permeabilities of these rocks have not been determined, and their suitability for thermoelectric power generation represents the greatest source of uncertainty in this analysis. For example, the Nugget Sandstone, where it produces oil and gas, has porosities ranging from ca. 5-25% and permeabilities that range over five orders of magnitude (ca. 0.05 mD to >1 Darcy; Lindquist, 1988). For this analysis, the thickness of potential reservoir rocks in both Area A and B has been conservatively estimated to range from 100 to 700 m, for a combined reservoir volume of 28 to 371 km^3 at depths of 3 to 4 km. In Area C, the 150 ^{o}C isotherm lies about a kilometer deeper (Figure 7), and is outside the economic temperature-depth envelope of Allis et al. (2013, 2015) and Allis and Moore (2014). The estimated thickness of potential reservoir rocks within this area also ranges from 100 to 700 m, but the estimated reservoir volume is much smaller, between 10 and 70 km^3. Because Area C's thermal resource lies at greater depth, higher drilling costs would be incurred, and if fluids at these depths prove to be highly saline (Welhan et al., 2014; Welhan, in review), then additional engineering and power production costs would accrue.

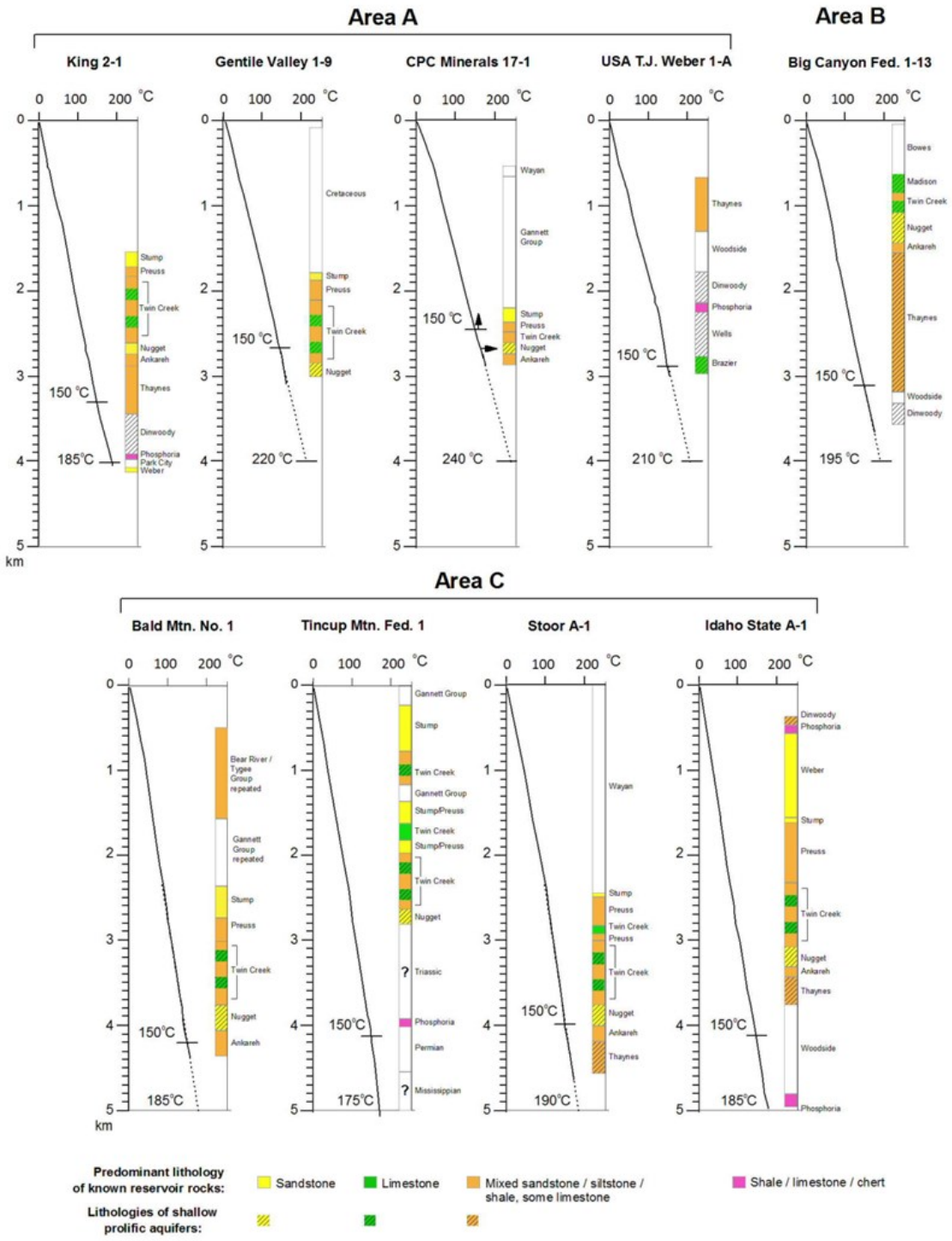

Figure 7: Summary of information on potential reservoir rocks and temperatures as constrained by deep-well data within the principal heat flow anomaly (Area A of Figure 6), in a single well having elevated heat flow (Area B), and wells of intermediate heat flow immediately south of the primary heat-flow anomaly (Area C). Wells in Areas A and B have economic temperatures exceeding 150 ºC between 3 and 4 km, whereas wells in Area C only achieve these temperatures between 4 and 5 km depth. Lithologies shown in color represent rocks known to host commercial oil and gas deposits in the thrust belt in general (Figure 3) and in northern Utah, in particular (UGS, 2009). Hatched symbology indicates formations with lithologies that host prolific shallow aquifers in the study area. Thermal profiles represent best-fit geotherms fitted to corrected BHTs and the formation-specific thermal conductivities of Welhan and Gwynn (2014).

Table 4 summarizes the range of reservoir temperatures, volumes, reservoir recovery and energy conversion factors that were used in the Monte Carlo analysis for the three areas. Note that, although reservoir temperatures in Area A range up to at least 240 ^{o}C, a conservative maximum of 200 ^{o}C was utilized for this analysis.

4.3 Power-Generation Potential

Six of the variables in Equation 5 have a considerable range of possible values, so a Monte Carlo parameter-selection approach was used to consider the interaction of these uncertainties on the resulting power estimates. The assumptions underlying this implementation of the Monte Carlo procedure are: (1) the uncertainties in all parameters are independent of each other; (2) parameter values have a uniform probability distribution between the assigned minimum and maximum values of Table 4; and (3) the reservoir volumetric heat capacity is fixed at 2450 kJ/kg ^{o}K. For each realization, values were selected at random from the parameter probability distributions to calculate a power-capacity estimate using Equation 5; the process was repeated for 20,000 realizations to produce a probability distribution of estimates for each scenario. The resulting probability distributions define the likely power-generation potential for each scenario considered, in terms of a mean, a median, and an interquartile range (IQR).

	Area A	Area B	Area C
Depth, km to 150 °C isotherm	2.8 ± 0.5	3.1 ± 0.5	4.3 ± 0.5
T, °C *	215 ± 15 (at 4 km)	195 ± 15 (at 4 km)	185 ± 15 (at 5 km)
T_{avg}, °C	185 ± 15 (at 2.5-4 km)	170 ± 15 (at 3-4 km)	170 ± 10 (at 4-5 km)
Reservoir ** thickness, m	400 ± 300 (at 2.5-4 km)	>400 (at 3-4 km)	400 ± 300 (at 4-5 km)

* by extrapolation of conductive gradient

** based on formations and lithologies of known reservoir quality actually encountered

Table 3: Reservoir temperatures and thicknesses inferred from thermal gradients and presence of known reservoir-quality formations (Figure 7). Area designations correspond to those defined in Figure 6.

Area A	T_R, °C *	V_R, km^3	n	R
Min	170	20	0.05	0.02
Max	200	350	0.12	0.10
Area B	**T_R, °C ***	**V_R, km^3**	**n**	**R**
Min	170	8	0.05	0.02
Max	200	21	0.12	0.10
Area C	**T_R, °C ***	**V_R, km^3**	**n**	**R**
Min	150	10	0.05	0.02
Max	170	70	0.08 **	0.10

* average temperatures between the 150 °C isotherm and either 4 km (Areas A, B) or 5 km (Area C)

** for binary-cycle power development of lower temperature and possibly high salinity fluid

Table 4: Summary of estimated reservoir temperatures and volumes, and ranges of energy conversion factor (n) and reservoir recovery factor (R) used to constrain parameter selection for the Monte Carlo analysis.

Power-generation capacity estimates were derived for each of Areas A, B and C and three rejection temperature scenarios: (1) T_o fixed at 15 ^oC; (2) T_o fixed at 40 ^oC; and (3) T_o uncertain within this range. The resulting distributions of estimated power-generation potential are summarized in **Figure 8** and in **Table 5**.

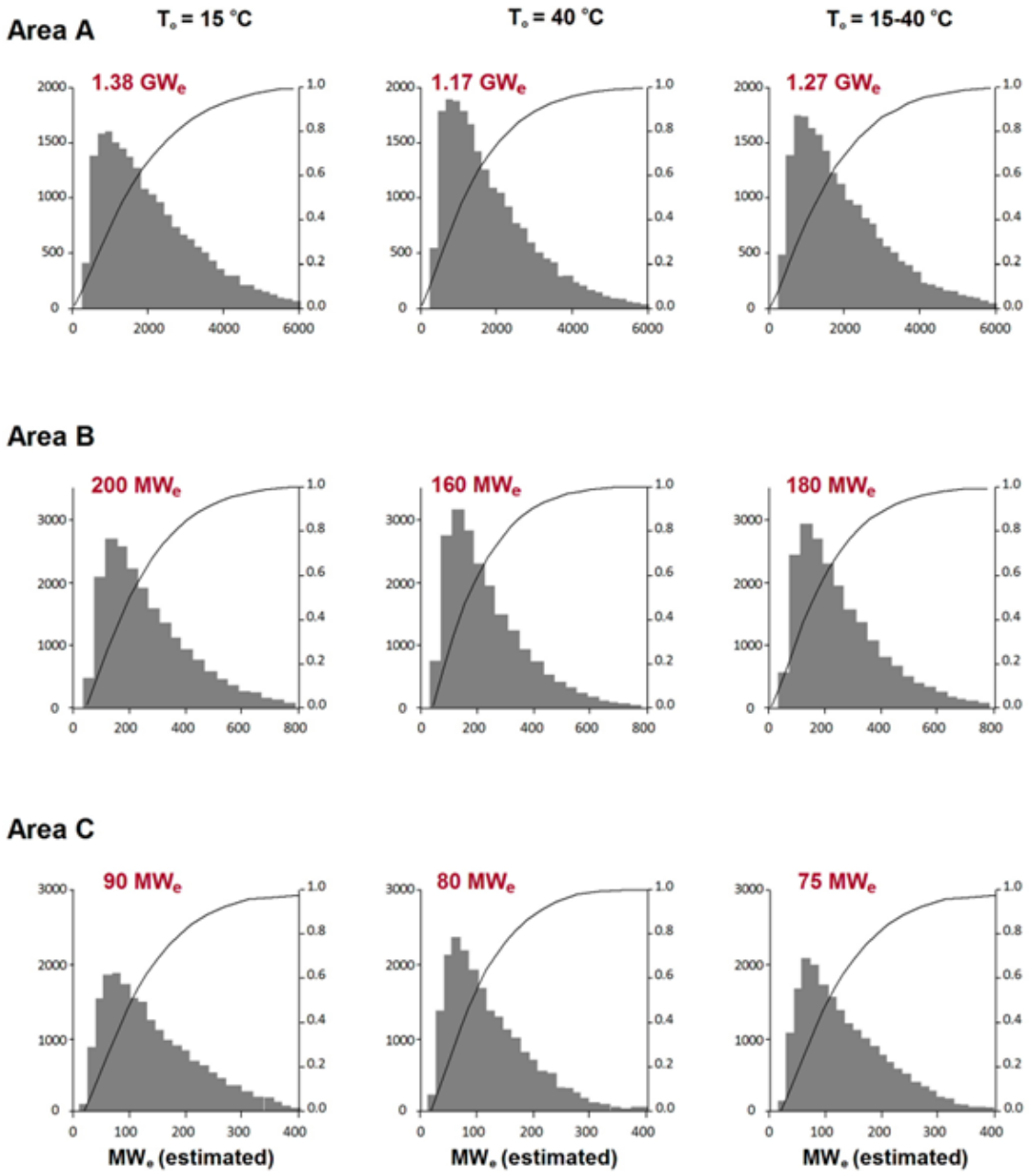

Figure 8: Monte Carlo estimates of power-generation potential for each area and for three rejection temperature scenarios: T_o fixed at 15 ^oC; at 40 ^oC; and a value that is uncertain within this range. Medians are shown in red font.

Area A	T_o = 15 °C	T_o = 40 °C	T_o = 15-40 °C
Mean	1670	1420	1550
Median	1380	1170	1270
IQR	1600	1350	1450
Min	48	43	55
Max	7471	6189	7046
Area B	T_o = 15 °C	T_o = 40 °C	T_o = 15-40 °C
Mean	230	190	210
Median	200	160	180
IQR	200	170	180
Min	18	14	16
Max	835	686	804
Area C	T_o = 15 °C	T_o = 40 °C	T_o = 15-40 °C
Mean	110	90	90
Median	90	80	75
IQR	94	79	78
Min	6	5	6
Max	423	383	372

Table 5: Summary of estimated power-generation potential in the three areas defined in Figure 6, for three rejection-temperature scenarios. All values are in MW_e. The summaries correspond to the probability distributions in Figure 8, each reflecting 20,000 Monte Carlo realizations of Equation 5. The interquartile range (IQR) provides a measure of the spread in estimates due to the interplay of parameter uncertainties in Table 4.

5. DISCUSSION

5.1 Power Potential of Areas A and B

The median power-generation potential within the primary heat flow anomaly (Area A) for a nominal 30-year life is of the order of 1.1 to 1.3 GW_e/year, based on rejection temperatures between 15 and 40 ^oC, power conversion factors typical of a flashed-steam process (0.05 - 0.12), and thermal recovery factors in the range of 0.02 - 0.10. For comparison, the GeoFRAT risk assessment tool (EGI, 2014), running 10,000 realizations with the parameter values in Table 4, produced a predicted 30-year power capacity of 2.0 GW_e/year. To some extent, GeoFRAT's higher predicted capacity reflects differences in its Monte Carlo assumptions, such as the use of triangular rather than uniform distributions, but the difference is principally due to the more conservative thermal recovery and power conversion factors utilized in the current evaluation.

Even considering the most conservative portion of the predicted power distribution, Area A is capable of producing 370 to 690 MW_e (10^{th} and 25^{th} percentiles, respectively; Figure 8). Its median power-generation estimates correspond to a reservoir power density of 2.3 to 5.5 MW_e/km^2 (for areas of 500 to 250 km^2, respectively), which is in the range predicted from simulations of idealized hot stratigraphic reservoirs (2 - 10 MW_e/km^2; Deo et al., 2014). Utilizing current geothermal power development assumptions with an initial reservoir temperature of 175 ^oC and a 1% per year temperature decline, Mines et al. (2014) demonstrated that the levelized cost of electricity generated in such systems is of the order of 10-15 cents/kWh.

However, reservoir rocks of the ITB may be more compartmentalized due to folding and faulting, relative to conventional sedimentary basin reservoirs, in which case, the thermal extraction efficiencies, thermal decline rates, and levelized costs could vary significantly among well fields developed in such a system.

Compared to Area A, the power-generating potential of Area B is a factor of five times lower, but its actual potential is essentially unknown because its area was arbitrarily set at 30 km^2 (Figure 6). Even at a minimum capacity of 160 to 200 MW_e, however, this area may have the best potential for near-term development because it lies less than 5 km from a major regional high-voltage transmission corridor and is within 25 km of the urban/mining center of Soda Springs, which utilizes considerable electric power processing ore from the region's phosphate mines (**Figure 9**).

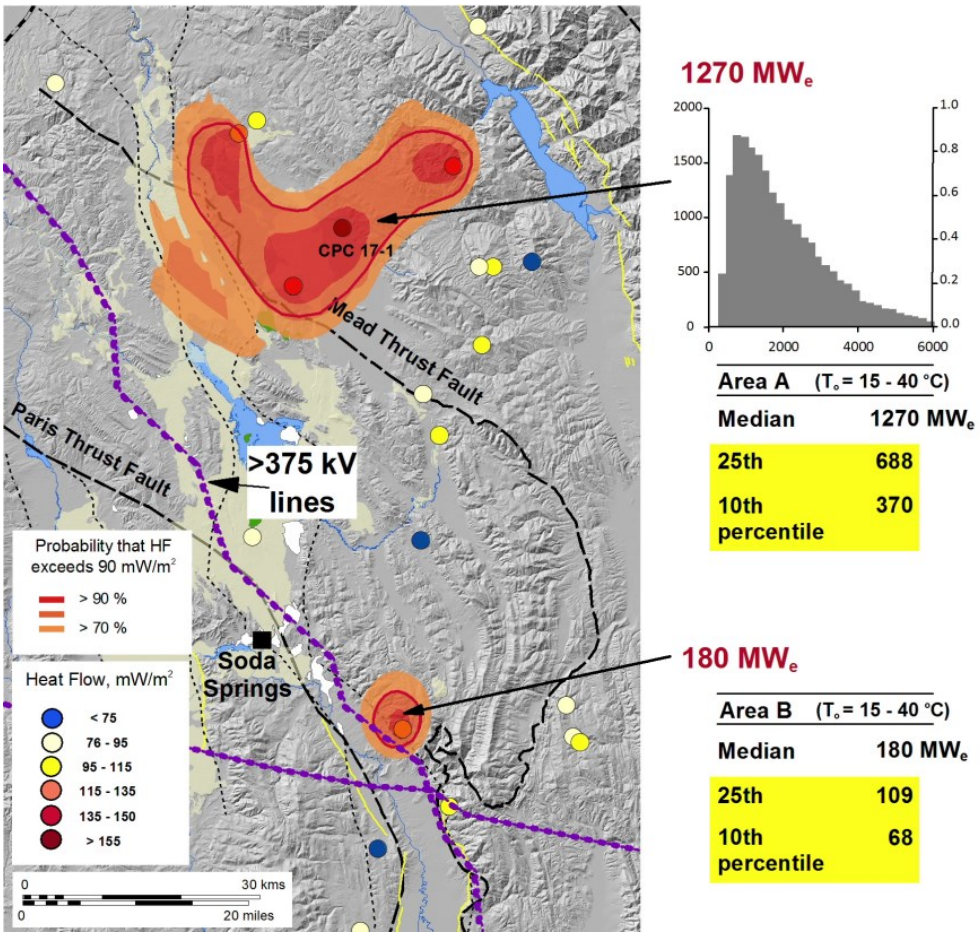

Figure 9: Summary of estimated power-generation potential in the two most promising areas of the Idaho thrust belt. Area A's minimum power potential, even at the 10 th or 25th percentiles of the predicted distribution is significant, although Area B may have higher near-term development potential because it lies within 5km of an existing transmission trunk line and within 25 km of Soda Springs, a major phosphate ore-smelting center.

5.2 Economic Potential of Area C

Because of its lower heat flow and reservoir temperatures (150 °C at 4 km vs. 195-215 °C in Areas A and B), greater depths necessary to achieve viable reservoir temperatures (4-5 km vs. 2.5-4 km), and potentially high fluid salinities (TDS up to 320,000 mg/l; Welhan et al., 2014; Welhan, in review), Area C's estimated power potential (75-90 MW_e) is likely marginal. First, these estimates are based on typical binary-process power conversion factors (0.05-0.08), but higher binary-process rejection temperatures may be necessary for these highly saline fluids (e.g., 60-80 °C; Kalinci et al., 2014). However, these lower-enthalpy reservoirs could be worthy of consideration, because their brines may host significant reserves of lithium (and other strategic elements?). Welhan et al. (2014) pointed out that a fluid sample collected in a deep drill stem test on a well in Area C (Idaho State A1; 3083 meters) had a lithium concentration of 113 mg/l, comparable to Salton Sea geothermal brines (Garret, 2004). If this reflects a hydrothermal contribution from this topaz-rhyolite magma due to a crystallization-driven lithium flux (estimated at ca. 100 tons /day; McCurry et al., 2014; 2015), then these hot, saline formation fluids may have co-production potential. If high lithium levels in the brines are confirmed, then these deeper thermal reservoirs may become economically attractive for their lithium co-production potential (e.g., Bourcier and Nix, 2003; Bloomquist, 2006).

6. CONCLUSIONS AND RECOMMENDATIONS

The results of this analysis confirm arguments of Allis et al. (2014, 2015), Allis and Moore (2014) and others that the sheer size of hot stratigraphically hosted geothermal resources can translate into considerable power-generation potential. A Monte Carlo analysis using the reservoir stored-heat method was conducted to estimate the electric power-generation potential of formation fluids hosted in known reservoir-quality rocks encountered in nine deep oil and gas exploration wells in the Idaho thrust belt. Three areas were evaluated, ranging from the hottest, shallowest wells in Areas A and B to the deepest, lowest-temperature, high-salinity wells in Area C.

The median estimated 30-year power generating potential of Area A is of the order of 1 GW_e, with power densities for the hottest and shallowest high-temperature reservoirs in Area A between 2.3 and 5.5 MW_e/km^2, similar to that estimated by Deo et al. (2014) for idealized hot stratigraphic reservoirs, and bracketing the 3 MW_e/km^2 baseline scenario considered in Allis and Moore's (2014)

simulations of hot stratigraphic reservoirs. Even considering the most conservative power estimates, Area A appears to be capable of producing 370 to 690 MW_e (10^{th} to 25^{th} percentile estimates, respectively). With a power potential estimated at 160-200 MW_e, Area B's proximity to existing transmission lines and a local market (phosphate ore-processing industry) may offer the best short-term potential for delineating and developing a commercial power plant. In comparison, Area C, with sub-economic reservoir temperature-depth conditions, lower heat flow and possible highly saline fluids, has the least power-generation potential and may not be worth further consideration unless new well data confirm the presence of potential lithium or other strategic mineral reserves in these brines.

Unlike conventional stratigraphically hosted geothermal resources, structural complexities in the Idaho thrust belt may reduce the thermal energy recovery efficiencies assumed in this analysis and possibly promote thermal drawdown in individual wells. Structurally compartmentalized reservoirs and short-range boundary effects will have to be assessed on a well-by-well basis. If high-salinity fluids are to be developed, then binary power-conversion options must be evaluated with regard to corrosion and scaling, and practical rejection temperatures will have to be optimized. Should dissolved lithium prove to be characteristic of these magmatically supported thermal fluids, then the engineering and environmental advantages of binary-cycle power extraction will have to be weighed against the economic returns from brine mineral extraction.

ACKNOWLEDGEMENTS

I thank Rick Allis and Joe Moore for discussions regarding the economic potential of hot stratigraphic reservoirs, which provided the impetus for performing this analysis. The work was wholly supported by the Idaho Geological Survey as an outcome of an analysis conducted during data compilation for the Department of Energy's National Geothermal Data System program.

REFERENCES

Allis, R., Blackett, R., Gwynn, M., Hardwick, C., Moore, J.N., Morgan, C., Schelling, D., and Sprinkel, D. 2012, Stratigraphic reservoirs in the Great Basin – the bridge to Enhanced Geothermal Systems in the U.S.; Geothermal Resources Council *Transactions*, v. 36, p. 351-357.

Allis, R., M. Gwynn, C. Hardwick, G. Mines, and J. Moore, 2015, Will Stratigraphic Reservoirs Provide the Next Big Increase in U.S. Geothermal Power Generation? Geothermal Resources Council *Transactions*, v. 39, p. 389-397.

Allis, R., Moore, J.N., Anderson, T., Deo, M., Kirby, S., Roehner, R., and Spencer, T., 2013, Characterizing the power potential of hot stratigraphic reservoirs in the Western U.S.; *Proceedings*, 38th Workshop on Geothermal Reservoir Engineering, Stanford University, p. 1463-1473.

Allis, R. and J. Moore, 2014, Can Deep Stratigraphic Reservoirs Sustain 100 MW Power Plants? Geothermal Resources Council, *Transactions*, v. 38, p. 1009-1016.

Bloomquist, R.G., 2006, Economic benefits of mineral extraction from geothermal brines; Washington State University Extension Energy Program, 6 pp.

Bourcier, W.L., M. Lin and G. Nix, 2003, Recovery of minerals and metals from geothermal fluids; 2003 SME Annual Meeting, Cincinnati, OH, Lawrence Livermore National Laboratory report UCRL-CONF-215135, 17 pp.

Brook, C.A., R.H. Mariner, D.R. Mabey, J.R. Swanson, M. Guffanti and L.J.P. Muffler, 1979, Hydrothermal Convection Systems With Reservoir Temperatures ≥ 90°C; *in* Assessment of Geothermal Resources of the United States – 1978, Muffler, L.J.P. (ed.), p. 18-85.

Deo, M., R. Roehner, R. Allis and J. Moore, 2014, Modeling of geothermal energy production from stratigraphic reservoirs in the Great Basin; *Geothermics*, v. 51, p. 3-45.

Franz, P., M. Neville-Lamb, L. azwar and J. Quinao, 2015, Calculation of geothermal stored heat from a numerical model for reserve estimation; *Proceedings*, World Geothermal Congress, Melbourne, Australia

Kalinci, Y., A. Hepbasli and I. Dincer, 2014, Exergetic performance assessment of a binary geothermal power plant; in Selcuk et al., eds., *Progress in Exergy, Energy, and the Environment*, Springer, New York, 1085 pp.

Lindquist, S.J., 1988, Practical characterization of eolian reservoirs for development: Nugget Sandstone, Utah-Wyoming thrust belt: Sedimentary Geology, v.56, p.315-339.

McCurry, M. and J.A. Welhan, 2012, Do Magmatic-Related Geothermal Energy Resources Exist in Southeast Idaho? Geothermal Resources Council *Transactions,* Vol. 36, p. 699-707.

McCurry, M., D.M. Pearson, J.A. Welhan, S.E. Kobs-Nawotniak, and Fisher, M.A., 2014, Origin and potential geothermal significance of China Hat and other late Pleistocene topaz rhyolite lava domes of the Blackfoot Volcanic Field, SE Idaho. Poster V33A-4830, Fall Meeting of the American Geophysical Union, San Francisco.

McCurry, M., D.M. Pearson, J.A. Welhan, S.E. Kobs-Nawotniak, and Fisher, M.A., 2015, Origin and potential geothermal significance of China Hat and other late Pleistocene topaz rhyolite lava domes of the Blackfoot Volcanic Field, SE Idaho: Geothermal Resources Council *Transactions* v.39, p.35-47.

Mendrinos, D., C. Karytsas and P.S. Georgilakis, 2008, Assessment of geothermal resources for power generation; *J. Optoelectronics and Advanced Materials*, v. 10, p. 1262-1267.

Mines, G., R. Allis, J. Moore and H. Hanson, 2014, Economics of Developing Hot Stratigraphic Reservoirs; Geothermal Resources Council *Transactions*, v. 38, p. 1047-1054.

Mitchell, J.C., L.L. Johnson and J.E. Anderson, 1980, Plate 1, Potential for Direct Heat Application of Geothermal Resources; Geothermal Investigations in Idaho, Part 9, *Water Information Bull*. 30, Idaho Dept. Water Resources, 396 pp.

Moon, H. and S.J. Zarrouk, 2012, Efficiency of geothermal power plants: a worldwide review; *Geothermics*, v. 51, p. 142–153.

Muffler, L. J. P., 1979, Assessment of Geothermal Resources of the United States—1978, U. S. Geological Survey Circular 790, 163 pp.

Nathenson, M., 1975, Physical factors determining the fraction of stored energy recoverable from hydrothermal convection systems and conduction-dominated areas; U.S. Geological Survey Open-File Report 75-525, 50 pp.

Sanyal, S.K. and Z. Sarmiento, 2005, Booking geothermal energy reserves; Geothermal Resources Council, *Transactions*, v. 29, p. 467-474.

Sanyal, S.K., R.C. Henneberger, C.W. Klein and R.W. Decker, 2002, A Methodology for Assessment of Geothermal Energy Reserves Associated with Volcanic Systems; Geothermal Resources Council *Transactions*, v. 26, p. 59-64.

Smith, R.L., H.R. Shaw, R.G. Luedke and S.L. Russell, 1978, Comprehensive tables giving physical data and thermal energy estimates for young igneous systems of the United States; U.S. Geological Survey Open-file report 78-925, 28 pp.

Smith, R.L. and H.R. Shaw, 1979, Igneous-related geothermal systems; *in* Assessment of Geothermal Resources of the United States – 1978, Muffler, L.J.P. (ed.), p.12-17.

UGS, 2009, Major Oil Plays in Utah and Vicinity; Utah Geol. Survey, Oil and Natural Gas Technology, Final Report, 605 pp. plus 6 plates.

Welhan, J.A., in review, Conceptual model and economic potential of a previously unrecognized high-temperature geothermal system in the Idaho thrust belt; Idaho Geological Survey, Technical Report and on-line data compendium.

Welhan, J.A., D. Garwood, and D. Feeney, 2013, The Blackfoot Volcanic Field, Southeast Idaho: A Hidden High-T Geothermal Resource Revealed Through Data Mining of the National Geothermal Data Repository; Geothermal Resources Council *Transactions*, v.37, pp.365-374.

Welhan, J.A., D. Garwood, and M.O. McCurry, 2013, The Blackfoot Volcanic Field, Southeast Idaho: A New Structural Paradigm for Hidden Geothermal Resources in the Northeastern Basin and Range; *AAPG Search and Discovery* #80329, AAPG Rocky Mountain Section Meeting, Salt Lake City, 18 pp.

Welhan, J.A. and M. Gwynn, 2014, High heat flow in the Idaho thrust belt: A hot sedimentary geothermal prospect: Geothermal Resources Council *Transactions*, v. 38., p. 1055-1066.

Welhan, J.A., M.L. Gwynn, S. Payne, M.O. McCurry, M. Plummer and T. Wood, 2014, The Blackfoot Volcanic Field, Southeast Idaho: A Hidden High-Temperature Geothermal Resource in the Idaho Thrust Belt; *Proceedings,* 39th Workshop on Geothermal Reservoir Engineering, Stanford University, Stanford CA SGP-TR-202, 13 pp.

Williams, C., Reed, M., and Mariner, R., 2008, A Review of the Methods Applied by the U.S. Geological Survey in the Assessment of Identified Geothermal Resources; U.S. Geological Survey Open-File Report 2008-1296, 27p.